

UCLA

UCLA Previously Published Works

Title

On-demand generation and mixing of liquid-in-gas slugs with digitally programmable composition and size

Permalink

<https://escholarship.org/uc/item/4xs9g9rp>

Journal

Journal of Micromechanics and Microengineering, 25(8)

ISSN

0960-1317

Authors

Chen, Yi-Chun
Liu, Kan
Shen, Clifton Kwang-Fu
[et al.](#)

Publication Date

2015-08-01

DOI

10.1088/0960-1317/25/8/084006

Peer reviewed



Published in final edited form as:

J Micromech Microeng. 2015 August ; 25(8): . doi:10.1088/0960-1317/25/8/084006.

On-demand generation and mixing of liquid-in-gas slugs with digitally-programmable composition and size

Yi-Chun Chen[†], Kan Liu^{†,‡}, Clifton Kwang-Fu Shen, and R. Michael van Dam^{*}

Department of Molecular & Medical Pharmacology and Crump Institute for Molecular Imaging, David Geffen School of Medicine, University of California, Los Angeles, 570 Westwood Plaza, Los Angeles, CA 90095

Abstract

Microscopic droplets or slugs of mixed reagents provide a convenient platform for performing large numbers of isolated biochemical or chemical reactions for many screening and optimization applications. Myriad microfluidic approaches have emerged for creating droplets or slugs with controllable size and composition, generally using an immiscible carrier fluid to assist with the formation or merging processes. We report a novel device for generation of liquid slugs in air when the use of a carrier liquid is not compatible with the application. The slug generator contains two adjacent chambers, each of which has a volume that can be digitally adjusted by closing selected microvalves. Reagents are filled into the two chambers, merged together into a contiguous liquid slug, ejected at the desired time from the device using gas pressure, and mixed by flowing in a downstream channel. Programmable size and composition of slugs is achieved by dynamically adjusting the volume of each chamber prior to filling. Slug formation in this fashion is independent of fluid properties and can easily be scaled to mix larger numbers of reagents. This device has already been used to screen monomer ratios in supramolecular nanoparticle assembly and radiolabeling conditions of engineered antibodies, and here we provide a detailed description of the underlying device.

Keywords

microfluidics; microchemistry; multiphase flow; slug generation; slug mixing; reaction optimization

Introduction

The advantages of performing reactions in microreactors, such as improved speed, selectivity, and safety, are well-documented in the literature [1–4]. These advantages are believed to arise in large part from the precise control of temperature, facilitated by the high surface to volume ratio in microfluidic devices. Using multiphase microfluidics, in which

^{*}Corresponding Author: R. Michael van Dam, mvandam@mednet.ucla.edu, 310-206-6507 (ph), 310-206-8975 (fax).

[†]These authors contributed equally to this work

[‡]Current address: College of Electronic and Electrical Engineering, Textile Industry Chain Collaboration Generic Technology Innovation Center, and Textile Materials and Advanced Processing Technology Hubei Province and the Ministry State Key Laboratory Breeding Base, Wuhan Textile University, Wuhan, China, 430075, P.R. China

droplets or slugs of one phase flow within a second carrier phase, further enhances this control over reaction conditions [5–8]. The movement of the droplet or slug causes an internal recirculating flow that increases the uniformity of its temperature and concentration [9]. Each droplet or slug in a multiphase system can be considered as an isolated, nanoliter-scale (or smaller) microreactor that in principle can be individually manipulated and analyzed. This microfluidic format is especially useful when working with scarce reagents, such as products of long chemical synthesis pathways, or isolated natural products that can only be obtained in small quantities. By creating droplets that each contain mixtures of a reagent with different samples, or by subjecting droplets to different reaction conditions, it is possible to perform extremely sample-efficient screening or optimization protocols. Investigators have capitalized on these advantages for many applications, such as screening enzyme inhibitors [10], screening protein crystallization conditions [11], screening chemical reaction conditions [12–15], optimizing supramolecular nanoparticle assembly [16], and optimizing radiolabeling conditions for antibody-based medical imaging agents [17].

Myriad microfluidic approaches exist for continuous generation of droplets and slugs comprising controlled amounts of reagents, generally at the junction of one or more reagent streams and an immiscible carrier stream [18–21]. In general, the size or composition of the slugs is determined by the flow parameters, and sequences of slugs with varying compositions can be created by controlling the flow parameters in a gradient manner [11]. To perform screens involving multiple different samples (e.g. enzyme inhibitors), typically the carrier stream is replaced with a pre-formed series of slugs of these samples, and the microfluidic junction injects additional reagents into each slug that passes by [8]. Amounts and identity of these added reagents may be constant or varied in a gradient manner.

While most early work focused on *continuous* generation of droplets and slugs, there has recently been tremendous interest in *on-demand* creation of slugs with programmable size and composition. This capability could improve reagent economy by enabling only selected reaction conditions to be tested, for example according to the principles of “design of experiments”. It also could pave the way to general-purpose fluidic devices for flexible mixing and processing of liquids at the nanoliter scale [22]. Injection of droplets or slugs of controllable size on demand has been demonstrated using laser pulses [23], off-chip valves [22,24], actuators affixed to microfluidic chips [25–27], on-chip micropumps [28], and on-chip microvalves [29–33]. Sizes of each slug are controlled by actuation duration. Increases in throughput can be achieved with multiple slug generators operating in parallel [24]. Mixtures of multiple reagents can be created by synchronized generation of pairs (or higher numbers) of single-reagent slugs, which are subsequently combined in downstream on-chip slug-merging structures. In one report, Lau *et al.* used a sophisticated on-chip “formulator” to prepare and mix a selected composition of several reagents prior to injection into the carrier stream [34]. In addition to on-demand creation of new slugs, there have been reports of on-demand injection of reagents into pre-existing slugs using microvalves [35] or electric fields [36].

In many applications the use of a carrier liquid is undesirable, due to difficulty in efficiently separating sample from the carrier liquid if additional processing is required, or due to the difficulty in finding a carrier fluid that is sufficiently immiscible with all reagents. Though

the use of a gaseous carrier is common in applications such as ink-jet printing and atomization, generation of droplets in air has not widely been used in microfluidic devices. Jiang *et al.* [37] demonstrated continuous generation of uniform water droplets in a gas stream, and on-demand generation of slugs in air has been achieved using microvalves. Sassa *et al.* [38] reported sophisticated manipulations of slugs in air and could generate different reaction mixtures by generating slugs of controlled amounts of individual reagents and merging them. We have previously reported a microvalve-based device to create liquid-in-air slugs with controllable composition of multiple reagents at the time of formation, i.e. without the need for additional slug manipulation steps [39]. In the device, the desired volumes of each reagent are loaded into adjacent chambers, followed by merging of the chamber contents and mixing by flowing the slug through the downstream microchannel.

We present here an improved liquid-in-air slug generator and mixer that is based on a similar principle but is more amenable to automation and user-friendly operation. Instead of controlling the filling pressure to determine the quantity of each reagent in an analog fashion, the quantity of each of multiple reagents is selected by digitally controlling the size of each chamber using microvalves. This simplifies the control system and the use of constant reagent loading pressure eliminates the problem of differing elastic expansion of each chamber, thereby eliminating the need for calibration of the device to account for the pressure-dependent expansion of PDMS [39]. This slug generation principle has already been reported for optimization of monomer ratios for supramolecular nanoparticle assembly [16], and optimization of radiolabeling conditions for antibody-based imaging agents [17]. The contribution of this paper is to describe the detailed design, theory of operation, and characterization of the device, as well as discuss the selection of parameters for automation of the device for generation and mixing of programmable slugs from arbitrary reagents.

Methods

Chip Design

We designed and fabricated a two-layer PDMS microfluidic chip (Figure 1) for generation of multi-component liquid-in-air slugs with programmable composition (Figure 2). The chip incorporates microvalves and pumps to control fluids [40] and leverages the permeability of PDMS for preparing well-defined volumes by blind filling of fixed-volume chambers [41]. The central feature of the design is a “slug generator”, comprising a long channel divided into two halves by a reagent isolation valve, V_{iso} . Each half is further subdivided into five equal chambers by individually-addressable volume-selection microvalves (V_{A1} , V_{A2} , V_{A3} , V_{A4} , V_{A5} for reagent A, and V_{B1} , V_{B2} , V_{B3} , V_{B4} , V_{B5} for reagent B). These valves can control the channel length (and therefore volume) that can be filled with each reagent. Note that the chambers closest to the central reagent isolation valve are slightly longer than the others; this is to compensate for the internal volume of the volume-selection valves and ensure the proper relative sizes of all chambers. Channels are approximately 200 μm wide by 40 μm deep, and each “unit volume” chamber has a length of 1.5 mm. A single chamber has a volume of approximately 6 nL. Upstream of the slug generator are three additional ports. One is used for controlling the pressure of chambers prior to filling, to decouple the slug ejection conditions (e.g. pressure of separation gas) from the slug generation process.

Typically this was used as a vent to reduce any trapped pressure to the atmospheric pressure. The second is used to flush the slug-generator and downstream channels with cleaning solution. The third is a peristaltic pump that admits controlled amounts of gas to eject the slugs into the mixing channel.

Our previous droplet generation devices directed all slugs to a single output for serial processing [39]. To facilitate applications of this device such as screening of radiochemical reaction conditions, or dispensing reagent combinations to off-chip instruments or assays (e.g. in well plates), a demultiplexer [42] is included in the chip design. This structure enables different slugs to be directed to different chip outlets for on-chip or off-chip analysis or processing, or allows extensive washing to be performed between samples in applications that are particularly sensitive to carryover. The demultiplexer uses $2 \cdot \log_2(N) = 6$ microvalves to direct the slug to 1 of $N=8$ different outlets. Demultiplexers can easily be scaled to much high numbers of outputs as demanded by the application.

Chip Fabrication

The microfluidic reaction optimization chip was implemented as a two-layer poly(dimethylsiloxane) (PDMS) chip according to common design and fabrication practices [39,40]. The upper layer of channels contains the fluidic channel network, consisting of reagent inlets, filling chambers, and slug output, while the lower layer contains microvalve control channels. Fabrication details have been described previously [39].

Chip Interface and Control System

To actuate an on-chip microvalve, the corresponding control channel was pressurized via a 3-way solenoid valve (SMC Series S070) connected to a 60 psig [414 kPag] nitrogen source. Microvalves were re-opened by venting the pressure. All valves were electronically-controlled through a data acquisition module (USB-4750, Advantech) by a software program written in LabView (National Instruments). Connections to control channels on the chip were made using 22 gauge stainless steel tubes inserted into punched holes in the chip, in turn connected to PTFE microbore tubing (0.022" ID, 0.042" OD, Cole-Parmer). Groups of 16 metal tubes were mounted into custom chip connectors developed in our lab to accelerate chip set-up and provide rigidity/stability to improve the maximum operating pressure of connections. Microvalve and pump control channels were filled with a small amount of hydraulic fluid (water) to avoid transfer of gas into the fluidic channels by permeation through the thin PDMS valve membrane. Water could be replaced by a low-viscosity mineral oil for applications where reagents in the fluidic channel are incompatible with water, or in applications such as chemical reactions involving high operating temperatures.

To the slug outlet channels, silica capillary tubing (75 μm ID, polyimide coated) was directly inserted. If Teflon or stainless steel tubing was used, we observed that the smallest slugs (6 nL) could not be reliably transferred from the chip into tubing without breaking apart.

Reagents A and B were loaded into GC vials connected to the chip via PTFE microbore tubing (0.012" ID, 0.030" OD, Cole-Parmer) inserted directly into the PDMS chip.

Nitrogen at pressure P_{fill} was applied to drive reagents into the chip to fill the chambers of the slug generator.

The inlet to the peristaltic pump (providing gas to eject slugs) was supplied with nitrogen at pressure P_{eject} .

Formation of Slugs

To generate a two-component slug (Figure 2), the two reagents, A and B, are driven by external pressure to blind fill the two chambers (A and B) in the slug-generation region of the chip. Each chamber is completely filled, the chamber volumes thus determining the volume of each of the two reagents that will comprise the slug. Contrary to our previous work where the amount of each liquid was determined by varying reagent driving pressure [39], here the size of each chamber is controlled digitally by microvalves. In the chip design we used here, the volume of each can be selected to be from 1-5 unit volumes (i.e., about 6-30 nL). For example, closing valve V_{A1} causes chamber A to be 1 unit volume in size; closing V_{A2} (but leaving V_{A1} open) causes chamber A to be 2 unit volumes in size; and so on. This selection is made immediately prior to the generation of the slug and is made independently for the two slugs.

On the fly, one can close appropriate valves to determine the volume of each reagent, thus affecting the slug size, reagent ratio, and relative concentration of each reagent (i.e. relative to original stock solution). Several examples are shown in Scheme 1 of Figure 3. For example, if the desired ratio of reagents A and B is 1:1 in a 2-unit slug, then valve V_{A1} and V_{B1} (Figure 2) are closed. If the desired ratio is 5:1 in a 6-unit slug, valve V_{A5} and valve V_{B1} are closed as shown in the third sequence. In some applications it is preferable to vary the amount of reagents but to keep the total slug volume constant. To facilitate this mode of operation, the chip design includes an extra pair of inlets for addition of buffer solutions (Scheme 2 of Figure 3). Reagent A and buffer A together occupy 5 unit volumes, and reagent B and buffer B together occupy 5 unit volumes. Scheme 3 of Figure 3 shows one additional way the slug generator can be operated. Reagents instead of buffer solutions are loaded into the end ports and the central ports are not used. A limitation is that all (10) chambers must be filled to avoid an air gap between reagents (which would prevent merging and mixing of the slug), but this scheme permits a wider range of reagent ratios, and a more uniform range of relative concentrations, than the other schemes. The Supplementary Information (Figure S5 and Tables S1-S3) illustrates the relationships among slug size, relative concentration of reagent A, and ratio of reagents A:B that can be achieved by the three schemes.

Ejection and Mixing of Slugs

After the chambers are filled up to the first closed volume-selection valve, their contents are isolated from the inlet channels (by closing valves V_A , V_B , $V_{\text{buf-A}}$, $V_{\text{buf-B}}$) and then merged by opening the reagent-isolation microvalve between them to form a single liquid slug with end-to-end reagent composition. This slug is pushed out of the slug-generation region with pressurized inert gas provided by a peristaltic pump to make room for the next slug. The action of driving the slug along the downstream channel causes its contents to mix [44]. In

our chip design, the mixing channel has sufficient length for completion of mixing before reaching the demultiplexer at the chip output.

Three valves were used as a peristaltic pump [40] to introduce controlled amounts of air to push newly-generated slugs out of the slug generator. (It should be noted that a total of six valves were incorporated into the design of the pump structure to provide additional flexibility in pumping parameters, but only three were used in this work.) The sequence of valves states used for peristaltic pumping is shown in the Supplementary Information (Figure S1). For a fixed pressure in the control channels and a fixed P_{eject} , each cycle pumps a fixed amount of nitrogen behind the most recently generated slug to move it out of the slug generation region. As the ejection gas expands to equilibrate with the pressure on the downstream side of the slug, the slug is pushed downstream. The slug is pushed to the output of the demultiplexer, enabling generation of the subsequent slug. The slug generator is vented prior to generation of the next slug in case any residual pressure remains in the filling chambers.

Once a multi-component liquid slug is generated, it is generally desirable to rapidly mix its contents and perform a physical or chemical process with well-defined residence time. Immediately downstream of the slug generator is a long serpentine channel for mixing. It has been shown that when droplets or liquid slugs are moved by pressure along a microchannel, an internal recirculating flow pattern is generated that mixes its contents within several slug lengths of movement [45,46][46]. In our chip, the mixing channel has been designed to be 5x the length of the longest slug that can be generated in the chip (10 unit volumes \approx 60 nL). The effectiveness of mixing in slugs has been shown to depend on the initial geometric configuration of reagents in the slug [47]. In the device presented here, slugs are always generated with axial (end-to-end) configuration of reagents thus they are optimally configured for mixing in simple, straight microchannels, and do not require meandering channels. Mixing of components of slugs with higher number of components (3 or 4) is achieved in the same fashion.

Characterization of Chip Operating Conditions

Chamber Filling—Because reagents are isolated from one another during the filling process, filling can be studied with only a single reagent. The time for a reagent to fill a chamber was measured as a function of (i) filling pressure and (ii) programmed chamber size (1 to 5 unit volumes). Additional variables not expected to affect filling time were also studied: (iii) reagent type, (iv) total reagent volume, and (v) ejection gas pressure.

For each characterization experiment, the reagent was loaded into a small vial, connected via tubing to the chip, and primed up to the inlet isolation valve, V_A . Filling pressure, chamber volume, and other parameters were adjusted according to the needs of the experiment. During the filling time, timestamped video was recorded (30 fps), and later analyzed to determine the duration of the filling process.

Slug Ejection—For a fixed ejection gas pressure, P_{eject} , of 10 psig [69 kPag], we measured the distance a slug moves as a function of the number of peristaltic pumping cycles. The distance the meniscus moved during different numbers of cycles was measured

by taking digital micrographs of the chip before and after the pumping cycle, and computing the distance using image analysis software. We observed the motion of a single slug as a function of number of pump cycles to verify the linearity of distance moved with number of pump cycles. Measurements were also performed with different slug sizes.

Carryover and Accuracy of Ratios—Accuracy of reagent ratios and carryover were measured by preparing slugs of radioactive [F-18]fluoride solution and deionized water. No-carrier-added [F-18]fluoride/[O-18]H₂O was produced by 11 MeV proton bombardment of 98 % enriched [O-18]H₂O in a silver target body using a RDS-112 cyclotron (Siemens). The [F-18]fluoride solution injected into the chip was prepared from 5 μ L of [F-18]fluoride/[O-18]H₂O and 1 μ L of 1M K₂CO₃.

We first measured the carryover from one slug to the next in order to determine a washing protocol. A 10 unit volume slug of [F-18]fluoride solution was generated and ejected to the first output channel. The liquid was captured in a glass capillary tube inserted into the channel output and then transferred to a gamma counter for radioactivity measurement. Next, several 10 unit volume slugs of deionized water were generated and ejected to the first output channel. Each wash slug was individually captured in a separate glass capillary tube and its radioactivity measured with a gamma counter (Wallac 1480 WIZARD 3). Measurements were corrected for radioactive decay and divided by the total collected radioactivity.

To measure accuracy of slug composition, 10-unit-volume slugs were generated using [F-18]fluoride solution as reagent A, deionized water as buffer A, and deionized water as reagent B (Scheme 2 of Figure 3). Slugs were generated with 0 to 5 unit volumes of [F-18]fluoride solution. Each was ejected, washed by a single 10-unit-volume slug of deionized water, and collected at output, and the radioactivity measured using a gamma counter. Radioactivity measurements were decay-corrected and were compared to the 1-unit-volume slug.

Results and Discussion

Determination of Operating Parameters for Automated Operation

An important design goal in this chip was to make the slug-generation process user-friendly and amenable to automation in a straightforward way. We aimed to make it possible to control the composition of every slug independently, despite the selected composition and despite the type of reagents used and their total volumes. We characterized the reagent filling time and slug ejection process in order to be able to choose one set of operating conditions that could be used for all generated slugs.

Selection of Slug Filling Parameters

The reagent-isolation valve V_{iso} separates the filling processes of the two reagents and thus the filling process can be studied by filling one half of the slug generator with one reagent.

In our previous work [39], we observed that filling a dead-end chamber occurs via a two-step process, characterized by an initial rapid increase to a non-zero filling fraction followed

by a much slower process during which the remainder of the chamber is filled. First, the pre-existing gas within the chamber is rapidly compressed until its pressure is in equilibrium with the pressure, P_{fill} , driving the reagent into the chamber. Assuming the ideal gas law applies, and there is no loss of gas and no temperature change, the initial volume V_0 of gas (at pressure P_0) shrinks to a smaller volume given by:

$$V' = \frac{P_0}{P_{\text{fill}}} V_0 \quad (1)$$

The chamber has a uniform cross-section, and assuming the channel cross-section is the same before and after filling, one can express the length of the chamber remaining empty as:

$$L' = \frac{P_0}{P_{\text{fill}}} L_0, \quad (2)$$

where L_0 is the initial chamber length. The timescale, t_1 , of this first compression phase is very short (on the order of 100 ms), with filling limited by the flow of reagent into the chamber to occupy the volume ($V_0 - V'$) previously occupied by gas. This flow depends on driving pressure (P_{fill}), geometry (size of microchannel and interconnect, length of pathway filled with fluid), and fluid viscosity.

In the second phase of the filling process, the compressed gas escapes the chamber by permeation through the PDMS matrix. The timescale, t_2 , of this phase is longer, and filling is limited by the escape of trapped gas. Permeation depends on the difference of pressure between the gas and its destination outside the chip, the permeability of PDMS to the trapped gas ($K_{\text{PDMS},\text{N}_2}$), and the geometry (thickness of the PDMS, and surface area through which the gas permeates). None of these factors is related to properties of the incoming reagent, and it is by using this portion of the filling process that we can ensure filling is independent of liquid properties.

Assuming permeation is a sufficiently slow process, we can assume the pressure of the trapped gas is constant, in equilibrium with P_{fill} . If we also assume the temperature remains constant and that the ideal gas law holds, we can write an expression for the change in molar amount (n) of remaining gas:

$$\frac{dn}{dt} = \frac{P_{\text{fill}}}{RT} \frac{dV}{dt} = \frac{P_{\text{fill}}}{RT} A \frac{dL}{dt} \quad (3)$$

where L is the length of the trapped gas segment and A is the cross-sectional area of the chamber. The molar loss due to permeation is given by

$$\frac{dn}{dt} = -\frac{1}{d} K_{\text{PDMS},N_2} (L(t)C + \varepsilon) (P_{\text{fill}} - P_{\text{ext}}) \quad (4)$$

where d is the thickness of PDMS through which the trapped gas is permeating, K_{PDMS,N_2} is the permeability of nitrogen in PDMS, $P_{\text{fill}} - P_{\text{ext}}$ is the difference in pressure between the trapped gas and the atmosphere outside the PDMS chip, C is the circumference of the chamber, and $LC + \varepsilon$ is the surface area through which nitrogen can permeate. We write $L = L(t)$ because the amount of remaining gas is a function of time, starting from an initial length L' (Equation 2) and ending at zero when the channel is completely filled. The term ε is included to avoid infinities during integration.

Combining Equations 3 and 4, and collecting constants into a new constant K , we obtain:

$$\frac{dL}{dt} = -\frac{RTK_{\text{PDMS},N_2}}{Ad} \frac{P_{\text{fill}} - P_{\text{ext}}}{P_{\text{fill}}} (L(t)C + \varepsilon) = -\frac{1}{K} \frac{P_{\text{fill}} - P_{\text{ext}}}{P_{\text{fill}}} (L(t)C + \varepsilon) \quad (5)$$

Integrating, we can compute the total time for the second phase of filling to be completed:

$$t_2 = -K \frac{P_{\text{fill}}}{P_{\text{fill}} - P_{\text{ext}}} \int_{L=L'}^{L=0} \frac{dL}{LC + \varepsilon} = \frac{K}{C} \frac{P_{\text{fill}}}{P_{\text{fill}} - P_{\text{ext}}} [\ln|LC + \varepsilon|]_0^{L'} = \frac{K}{C} \frac{P_{\text{fill}}}{P_{\text{fill}} - P_{\text{ext}}} \ln \left(\frac{L' C}{\varepsilon} + 1 \right)$$

and finally,

$$t_2 = \frac{K}{C} \frac{P_{\text{fill}}}{P_{\text{fill}} - P_{\text{ext}}} \ln \left(\frac{L_0 C}{\varepsilon} \frac{P_0}{P_{\text{fill}}} + 1 \right) \quad (6)$$

Empirically, this second phase is much slower than the first (compression) phase, and is limited by the permeation of air through the PDMS material of the chip. The slow speed limits the importance of viscous effects and this filling phase was expected to be independent of such factors as liquid properties, and total volume of liquid samples. Indeed, filling times were compared for water (viscosity, $\eta = 1$ mPa-s) and glycerol ($\eta = 1200$ mPa-s) and found to be identical within experimental error (data not shown) despite the large difference in viscosity. In addition, despite very large difference in fluidic resistance, we observed that total reagent volumes from 2 μL (a short slug within the inlet tubing) to 2 mL (the inlet tubing between the chip and reagent vial completely filled) exhibited virtually no difference in filling time when driven at the same pressure P_{fill} (Supplementary Information, Figure S2). Venting the filling chambers after each slug is ejected ensures P_0 is constant and removes dependence of filling time on P_{eject} (Supplementary Information, Figure S3).

The important dependencies in Equation 6 are the filling pressure, P_{fill} , and the initial volume/length of the chamber, L_0 . Thus, in order to determine optimal operating parameters, we characterized the filling time as a function of filling pressure, P_{fill} , and chamber volume (1 to 5 units, i.e. 6-30 nL) as shown in Figure 4. The data is in good agreement with the model of Equation 6. (See Supplementary Information for details of non-linear regression fitting.) This model could help predict operating parameters for chips with different geometries, different numbers of unit volumes, or even fabricated from different materials. To simplify automated operation, we selected a fixed filling time of 60 s that was sufficient to fill the maximum volume (5 unit volumes) at the selected filling pressure, $P_{\text{fill}} = 20$ psig [138 kPag]. This pressure provides a good compromise between filling speed (faster at higher pressures) and reliability of chip tubing interconnects and connections to reagent vials (more reliable at lower pressures).

Though the filling time is adequate for many applications where only modest number of slugs are needed (e.g., optimization of radiolabeling conditions [17]), there may be applications where a higher slug-generation rate, and faster filling time, is needed. There are several ways this could be achieved. For example, permeation of air out of the chambers could be enhanced by reducing the chip thickness or by placing vacuum channels in close proximity to the filling chambers, multiple slug generators could be operated in parallel, or initial pressure (P_0) of trapped air could be reduced by applying vacuum prior to filling. Though not studied in detail, reduction of P_0 increases the amount of liquid loaded during the initial filling phase, and decreases the amount of air ($L'A$) that needs to be eliminated during the second filling phase, resulting in filling times on the order of seconds. Another approach that could be used if some dependence on fluid properties is acceptable is to use a variation of our previous partial filling technique that depends on the initial (fast) part of chamber filling [39], however, instead of dynamically adjusting filling pressures for each reagent to control slug composition, the pressures can be held constant and the chamber sizes can be adjusted to achieve the desired filling amounts for each reagent.

Selection of Slug Ejection Parameters—Slugs were ejected from the slug generator by admitting pressurized gas via a peristaltic pump. In our previous work [39], we used a single valve to open a constant pressure source to move slugs, but we found that the sudden pressure change could cause fragmentation of liquid slugs, leading to substantial loss of the slug contents along the microchannel and tubing walls. In the present design, the peristaltic pump admits only small pulses of gas that more gently build-up pressure and accelerate the slug. Furthermore, peristaltic pumps permit the volume of added gas to be metered, enabling predictable positioning of slugs in the downstream channel. Each cycle of the peristaltic pump pushes a volume of pressurized gas from the pressurized gas source toward the slug. This gas expands, causing the slug to move until the pressure on both sides is equilibrated.

The distance moved that a slug moved per pumping cycle was found to depend linearly on the number of pumping cycles, but was dependent on the size of the slug (data not shown). This dependence is likely due to some leakage of the pressurized gas through the PDMS material. Because longer slugs have higher fluidic resistance, it takes longer to accelerate/move them, allowing increased leakage of gas and thus decreased total distance moved for a given amount of gas admitted by the peristaltic pump.

In some applications, slugs are pumped all the way to the output port. This would be useful if it is desired that all slugs experience the same amount of time in this part of this chip (e.g. if there are heat sources for performing chemical or biochemical reactions) and could be accomplished by determining the number of pump cycles needed to move the maximum size slug all the way to the output ports. Based on an ejection gas pressure of 10 psig [69.0 kPag] and a pump frequency of 2.5 Hz, 30 cycles were used to move slugs all the way to the outlet ports of the chip. These same parameters were used regardless of the slug size. Alternatively, in some applications, it may be desirable to direct all slugs to the same output port, and then it is only necessary for slugs to be pumped out of the slug generation region to make room for creation of the next slug. However, in this situation, the slug motion is less predictable and uniform because the total fluidic resistance depends not only on the newly formed slug but also any other slugs still in the mixing channel (or output tubing). We did observe that the distance that newly-generated slugs move for a fixed number of pumping cycles was strongly dependent on the number of slugs already in the mixing channel (data not shown).

Qualitative Verification of Mixing

Because slug mixing has been extensively studied in the literature, we sought only a qualitative verification that the slugs were being mixed within the length of the mixing channel. In Figure 5, a slug of 2 components (water with different colors of food dye) is generated and pumped through the mixing channel. The distinct colors in the original slug are observed to reach a homogeneous mixture during its transit through the mixing channel.

On-the-fly Selection of Compositions

Liquid-in-air slugs with digitally programmable composition were generated on demand using the filling parameters (pressure and time) determined above. To generate slugs of different compositions, no operating parameters were changed – the computer program simply controlled the closure of particular chamber size selection valves depending on the desired composition. Figures 6a and 6b show sequences of slugs inside the chip, where each slug has a unique but well-defined size and composition, generated from Scheme 1 of Figure 3. Slugs exhibit uniform appearance suggesting rapid mixing and their length and color reflects the expectation based on composition. It can also be observed that none of the slugs were fragmented and that there is negligible residue between slugs. Furthermore the change in slug composition is instantaneous: there are no wasted “intermediate” slugs when switching from one size/composition to another.

Quantitation of Carryover and Volume Accuracy

Since the generated slugs make contact with the channel walls there is a possibility of contamination. Using radioactive solutions, we measured the carryover from one slug to the next. After generating a slug of [F-18]fluoride solution, 1.5% of the radioactivity was found in the immediately subsequent slug of water, and 0% in additional slugs (Supplementary Information, Figure S4). Therefore a single slug (10 unit volumes) of water could be used to effectively wash the chip. The low loss from the initial slug suggests that the amount lost during slug flow will at most affect the reagent ratio of the next slug by 1.5%, assuming preferential loss of one reagent but not the other.

Using this wash protocol, the accuracy of volume ratios in the generated slugs was investigated with radioactive solutions. Ratios of radioactivity in the slugs generated with different amounts of [F-18]fluoride solution were compared to the first slug and show the expected linear relationship (Figure 7), with an error <2% between the actual and expected values.

Applications of Programmable Slug-Generation

Digitally-programmed slug generation has been used for optimization of monomer ratios for supramolecular nanoparticle assembly [16], and for optimization of radiolabeling conditions for antibody-based imaging agents [17]. In the latter application, the effect of the ratio of the labeling agent N-succinimidyl-4-[F-18]fluorobenzoate ([F-18]SFB) to an anti-PSCA diabody was explored. Each individual slug had sufficient material for analysis of labeling yield enabling optimization with miniscule reagent consumption. In fact, this study consumed 4-5 orders of magnitude less protein per data point compared with conventional macroscale studies, requiring on average only 41 ng of protein (for 2.0 mg/mL stock) per data point. Once optimal conditions were determined, larger amounts could be produced at the optimal yield by generating and pooling a large number of slugs with identical composition. Automation was especially important in this application because it was necessary to operate the chip behind lead shielding where it is difficult to find space for observation equipment such as microscopes, and because the optimization process needs to be performed routinely due to difficult-to-measure batch-to-batch variations in the radiolabeling agent or the biomolecule. In addition to other types of reaction optimization experiments with scarce reagents, the chip could be used for dispensing/formulating mixtures of radiolabeled compounds or drugs for chip-based cell studies.

Conclusions

We have developed a PDMS-based screening and reaction optimization chip based on programmable generation of liquid-in-gas slugs. Size and composition of 2, 3, or 4-component slugs can be digitally controlled. The use of microvalves decouples the liquids as the slug is formed, avoiding effects such as change in reagent orientation as a function of viscosity [47], and allows dynamic control of the volume of each reagent during slug formation. The chip has been designed so the slug-creation time and slug-ejection times can easily be predicted and therefore can be readily automated. Slug generation time was determined to be independent of reagent type, total reagent volume, and other factors. This enables worry-free operation, with reliable slug generation despite variations in a wide range of parameters. Unlike our previous work [39], ratios of reagents are limited to discrete rather than continuous values. This does not represent a practical limitation since optimization studies are generally performed by choosing discrete values for a parameter over a range of interest. The chip design could be scaled to larger numbers of chambers to achieve higher resolution of reagent concentrations. Advantages of this new approach include removing the dependence of optimal filling time on viscosity, eliminating the need for rapidly controlling pressures, and eliminating the need for calibration of each chip (e.g., due to batch-to-batch variations in PDMS). The use of a peristaltic pump to more gently eject slugs and avoid breakup was also helpful in working with individual slugs.

Supplementary Material

Refer to Web version on PubMed Central for supplementary material.

Acknowledgments

This work was supported in part by the National Cancer Institute (Nanosystems Biology Cancer Center, grant number U54CA119347-01), the Industry-University Cooperative Research Program (UC Discovery Grant number bio07-10665) and a project development grant from the UCLA Center for In Vivo Imaging in Cancer Biology (National Institutes of Health Grant number 5P50CA086306). The authors thank Dirk Williams and Darin Williams for assistance in designing and fabricating custom chip connectors.

References

1. Wiles C, Watts P. Continuous Flow Reactors, a Tool for the Modern Synthetic Chemist. *Eur J Org Chem.* 2008; 2008:1655–71.
2. Arima, V., Watts, P., Pascali, G. Microfluidics in Planar Microchannels: Synthesis of Chemical Compounds On-Chip. In: Castillo-León, J., Svendsen, WE., editors. *Lab-on-a-Chip Devices and Micro-Total Analysis Systems.* Springer International Publishing; 2015. p. 197-239.
3. McMullen JP, Jensen KF. Integrated Microreactors for Reaction Automation: New Approaches to Reaction Development. *Annual Review of Analytical Chemistry.* 2010; 3:19–42.
4. Brivio M, Verboom W, Reinhoudt D. Miniaturized continuous flow reaction vessels: influence on chemical reactions. *Lab Chip.* 2006; 6:329–44. [PubMed: 16511615]
5. Zhao S, Wang W, Shao T, Zhang M, Jin Y, Cheng Y. Mixing performance and drug nano-particle preparation inside slugs in a gas–liquid microchannel reactor. *Chemical Engineering Science.* 2013; 100:456–63.
6. Köhler, JM., Cahill, B. *Micro-Segmented Flow: Applications in Chemistry and Biology.* Springer Science & Business Media; p. 2013
7. Günther A, Jensen KF. Multiphase microfluidics: from flow characteristics to chemical and materials synthesis. *Lab Chip.* 2006; 6:1487–503. [PubMed: 17203152]
8. Song H, Chen DL, Ismagilov RF. Reactions in Droplets in Microfluidic Channels. *Angew Chem Int Ed.* 2006; 45:7336–56.
9. Köhler JM, Li S, Knauer A. Why is Micro Segmented Flow Particularly Promising for the Synthesis of Nanomaterials? *Chemical Engineering & Technology.* 2013; 36:887–99.
10. Sun S, Slaney TR, Kennedy RT. Label Free Screening of Enzyme Inhibitors at Femtomole Scale Using Segmented Flow Electrospray Ionization Mass Spectrometry. *Anal Chem.* 2012; 84:5794–800. [PubMed: 22656268]
11. Zheng B, Roach LS, Ismagilov RF. Screening of Protein Crystallization Conditions on a Microfluidic Chip Using Nanoliter-Size Droplets. *J Am Chem Soc.* 2003; 125:11170–1. [PubMed: 16220918]
12. Hatakeyama T, Chen DL, Ismagilov RF. Microgram-Scale Testing of Reaction Conditions in Solution Using Nanoliter Plugs in Microfluidics with Detection by MALDI-MS. *Journal of the American Chemical Society.* 2006; 128:2518–9. [PubMed: 16492019]
13. De Bellefon C, Tanchoux N, Caravieilhés S, Grenouillet P, Hessel V. Microreactors for Dynamic, High Throughput Screening of Fluid/Liquid Molecular Catalysis. *Angew Chem Int Ed.* 2000; 39:3442–5.
14. Garcia-Egido E, Spikmans V, Wong SYF, Warrington BH. Synthesis and analysis of combinatorial libraries performed in an automated micro reactor system. *Lab Chip.* 2003; 3:73. [PubMed: 15100785]
15. Gong X, Miller PW, Gee AD, Long NJ, de Mello AJ, Vilar R. Gas–Liquid Segmented Flow Microfluidics for Screening Pd-Catalyzed Carbonylation Reactions. *Chem Eur J.* 2012; 18:2768–72. [PubMed: 22331821]

16. Liu K, Wang H, Chen KJ, Guo F, Lin WY, Chen YC, Phung DL, Tseng HR, Shen CKF. A digital microfluidic droplet generator produces self-assembled supramolecular nanoparticles for targeted cell imaging. *Nanotechnology*. 2010; 21:445603. [PubMed: 20935351]
17. Liu K, Lepin EJ, Wang MW, Guo F, Lin WY, Chen YC, Sirk SJ, Olma S, Phelps ME, Zhao XZ, Tseng HR, van Dam RM, Wu AM, Shen CF. Microfluidic-based ¹⁸F-Labeling of Biomolecules for Immuno-Positron Emission Tomography. *Mol Imag*. 2011; 10:168–76.
18. Christopher GF, Anna SL. Microfluidic methods for generating continuous droplet streams. *J Phys D: Appl Phys*. 2007; 40:R319.
19. Teh SY, Lin R, Hung LH, Lee A. Droplet microfluidics. *Lab on a Chip*. 2008; 8:198–220. [PubMed: 18231657]
20. Seemann R, Brinkmann M, Pfohl T, Herminghaus S. Droplet based microfluidics. *Rep Prog Phys*. 2012; 75:016601. [PubMed: 22790308]
21. Sharma, S., Srisa-Art, M., Scott, S., Asthana, A., Cass, A. Droplet-Based Microfluidics. In: Jenkins, G., Mansfield, CD., editors. *Microfluidic Diagnostics Methods in Molecular Biology*. Humana Press; 2013. p. 207-30.
22. Tangen U, Sharma A, Wagler P, McCaskill JS. On demand nanoliter-scale microfluidic droplet generation, injection, and mixing using a passive microfluidic device. *Biomicrofluidics*. 2015; 9:014119. [PubMed: 25759752]
23. Park SY, Wu TH, Chen Y, Teitell MA, Chiou PY. High-speed droplet generation on demand driven by pulse laser-induced cavitation. *Lab Chip*. 2011; 11:1010–2. [PubMed: 21290045]
24. Guzowski J, Korczyk PM, Jakiela S, Garstecki P. Automated high-throughput generation of droplets. *Lab Chip*. 2011; 11:3593–5. [PubMed: 21927762]
25. Churski K, Michalski J, Garstecki P. Droplet on demand system utilizing a computer controlled microvalve integrated into a stiff polymeric microfluidic device. *Lab Chip*. 2010; 10:512–8. [PubMed: 20126693]
26. Xu J, Attinger D. Drop on demand in a microfluidic chip. *J Micromech Microeng*. 2008; 18:065020.
27. Gu W, Zhu X, Futai N, Cho BS, Takayama S. Computerized microfluidic cell culture using elastomeric channels and Braille displays. *Proceedings of the National Academy of Sciences of the United States of America*. 2004; 101:15861–6. [PubMed: 15514025]
28. Zeng Y, Shin M, Wang T. Programmable active droplet generation enabled by integrated pneumatic micropumps. *Lab Chip*. 2012; 13:267–73. [PubMed: 23160148]
29. Bontoux N, Pépin A, Chen Y, Ajdari A, Stone HA. Experimental characterization of hydrodynamic dispersion in shallow microchannels. *Lab Chip*. 2006; 6:930. [PubMed: 16804598]
30. Sun X, Tang K, Smith RD, Kelly RT. Controlled dispensing and mixing of pico- to nanoliter volumes using on-demand droplet-based microfluidics. *Microfluid Nanofluid*. 2013; 15:117–26. [PubMed: 23935562]
31. Guo F, Liu K, Ji XH, Ding HJ, Zhang M, Zeng Q, Liu W, Guo SS, Zhao XZ. Valve-based microfluidic device for droplet on-demand operation and static assay. *Applied Physics Letters*. 2010; 97:233701.
32. Zeng S, Li B, Su X, Qin J, Lin B. Microvalve-actuated precise control of individual droplets in microfluidic devices. *Lab Chip*. 2009; 9:1340–3. [PubMed: 19417898]
33. Lin R, Fisher JS, Simon MG, Lee A. Novel on-demand droplet generation for selective fluid sample extraction. *Biomicrofluidics*. 2012; 6:024103–024103–10.
34. Lau BTC, Baitz CA, Dong XP, Hansen CL. A Complete Microfluidic Screening Platform for Rational Protein Crystallization. *Journal of the American Chemical Society*. 2007; 129:454–5. [PubMed: 17226984]
35. Zec H, Rane TD, Wang TH. Microfluidic platform for on-demand generation of spatially indexed combinatorial droplets. *Lab Chip*. 2012; 12:3055–62. [PubMed: 22810353]
36. Abate AR, Hung T, Mary P, Agresti JJ, Weitz DA. High-throughput injection with microfluidics using picoinjectors. *PNAS*. 2010; 107:19163–6. [PubMed: 20962271]
37. Jiang K, Lu AX, Dimitrakopoulos P, DeVoe DL, Raghavan SR. Microfluidic Generation of Uniform Water Droplets Using Gas as the Continuous Phase. *Journal of Colloid and Interface Science*.

38. Sassa F, Fukuda J, Suzuki H. Microprocessing of Liquid Plugs for Bio/chemical Analyses. *Analytical Chemistry*. 2008; 80:6206–13. [PubMed: 18627178]
39. Liu K, Chen YC, Tseng HR, Shen CKF, Dam RM. Microfluidic device for robust generation of two-component liquid-in-air slugs with individually controlled composition. *Microfluid Nanofluid*. 2010; 9:933–43. [PubMed: 20930933]
40. Unger MA, Chou HP, Thorsen T, Scherer A, Quake SR. Monolithic Microfabricated Valves and Pumps by Multilayer Soft Lithography. *Science*. 2000; 288:113–6. [PubMed: 10753110]
41. Hansen CL, Skordalakes E, Berger JM, Quake SR. A robust and scalable microfluidic metering method that allows protein crystal growth by free interface diffusion. *Proceedings of the National Academy of Sciences of the United States of America*. 2002; 99:16531–6. [PubMed: 12486223]
42. Melin J, Quake SR. Microfluidic Large-Scale Integration: The Evolution of Design Rules for Biological Automation. *Annu Rev Biophys Biomol Struct*. 2007; 36:213–31. [PubMed: 17269901]
43. Eddings MA, Johnson MA, Gale BK. Determining the optimal PDMS–PDMS bonding technique for microfluidic devices. *Journal of Micromechanics and Microengineering*. 2008; 18:067001.
44. Günther A, Jhunjhunwala M, Thalmann M, Schmidt MA, Jensen KF. Micromixing of Miscible Liquids in Segmented Gas-Liquid Flow. *Langmuir*. 2005; 21:1547–55. [PubMed: 15697306]
45. Rhee M, Burns MA. Drop Mixing in a Microchannel for Lab-on-a-Chip Platforms. *Langmuir*. 2008; 24:590–601. [PubMed: 18069861]
46. Dogan H, Nas S, Muradoglu M. Mixing of miscible liquids in gas-segmented serpentine channels. *International Journal of Multiphase Flow*. 2009; 35:1149–58.
47. Tice JD, Lyon AD, Ismagilov RF. Effects of viscosity on droplet formation and mixing in microfluidic channels. *Analytica Chimica Acta*. 2004; 507:73–7.

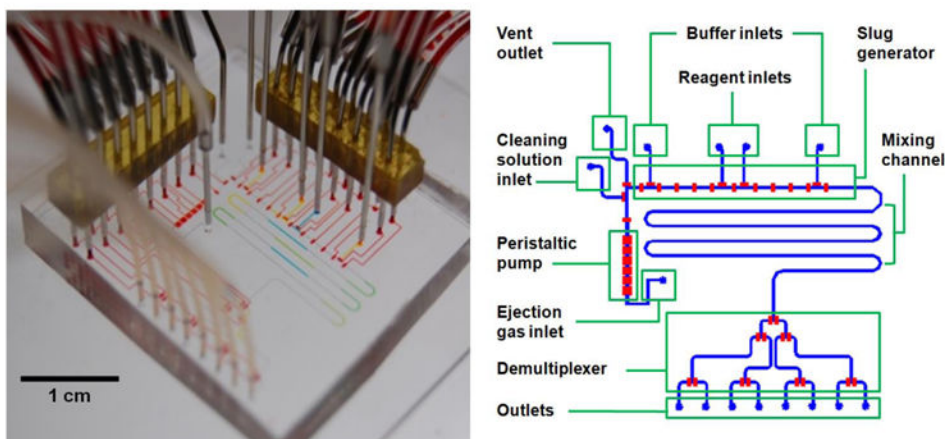


Figure 1. (Left) Photograph of slug generation and mixing chip for reaction optimization. Channels are filled with food dye for purposes of visualization: microvalve control channels (red), reagent A (yellow), reagent B (blue). (Right) Schematic of chip design illustrating the various functional components. The fluid layer is shown in blue and the control layer in red. For clarity, only the microvalves (red rectangles) are shown in the control layer.

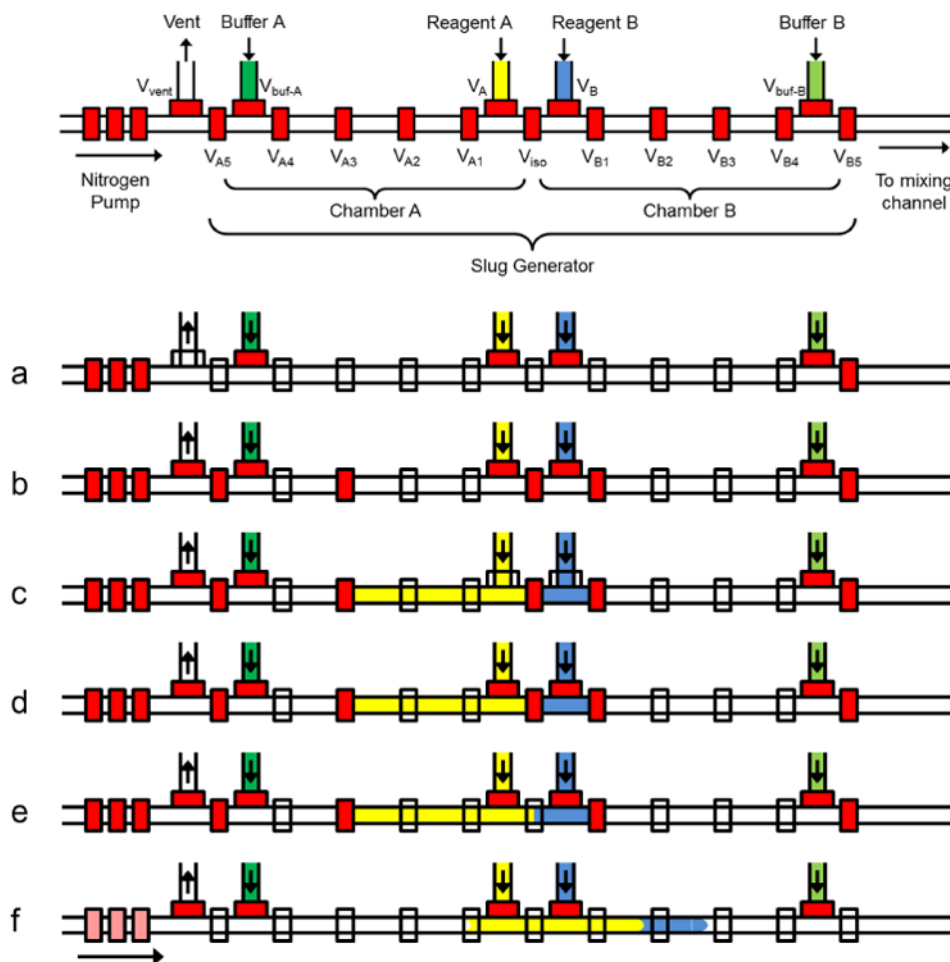


Figure 2. (Top) Schematic of slug generator, vent port and nitrogen pump. Microvalves are represented by red rectangles and labeled with names used in the text. (Bottom) Sequence of steps to generate a slug. (a) Vent is opened to release any residual pressure in channel. (b) Chamber size is adjusted by closing appropriate valves. In this case, a 3:1 (A:B) slug is shown. (c) Chambers are filled with reagents. If buffer solutions are used, they would also be filled at this time. (d) Filled chambers are sealed. (e) Adjacent chambers are merged by opening isolation valve. If buffer solutions are used, the contents of buffer-filled chambers would be merged into the slug as well. (f) Slug is ejected with nitrogen pump to the selected demultiplexer output. The slug mixes as it flows.

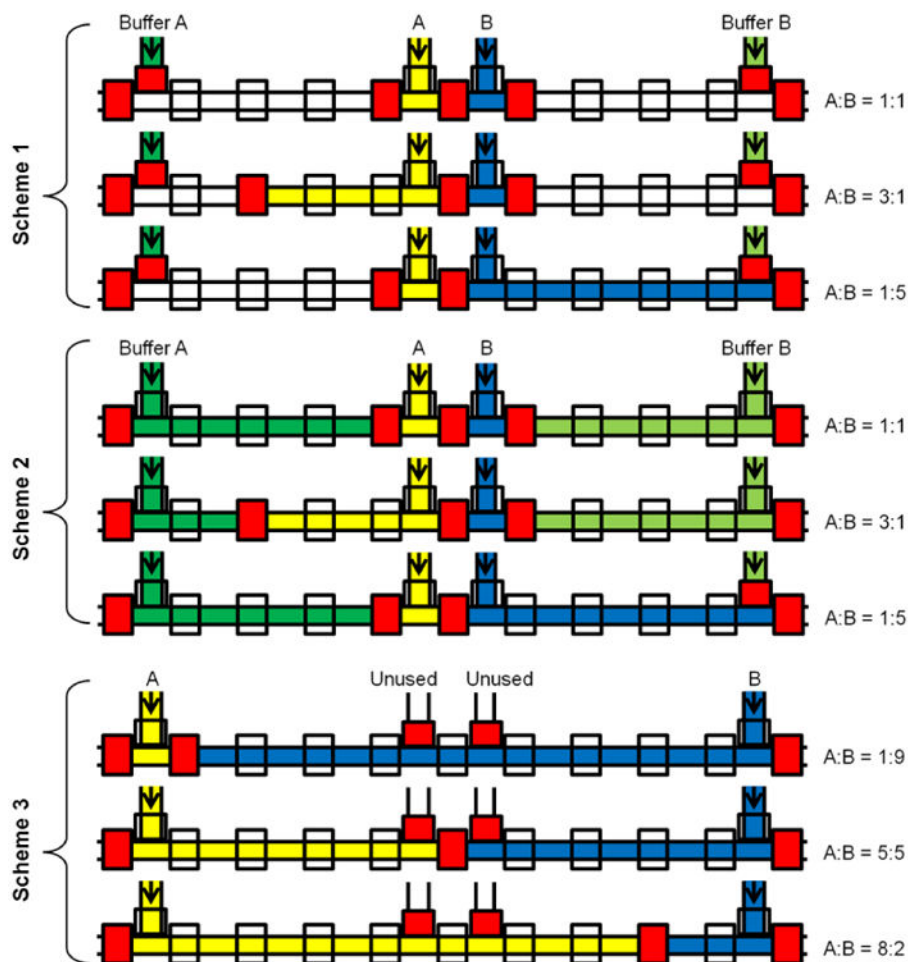
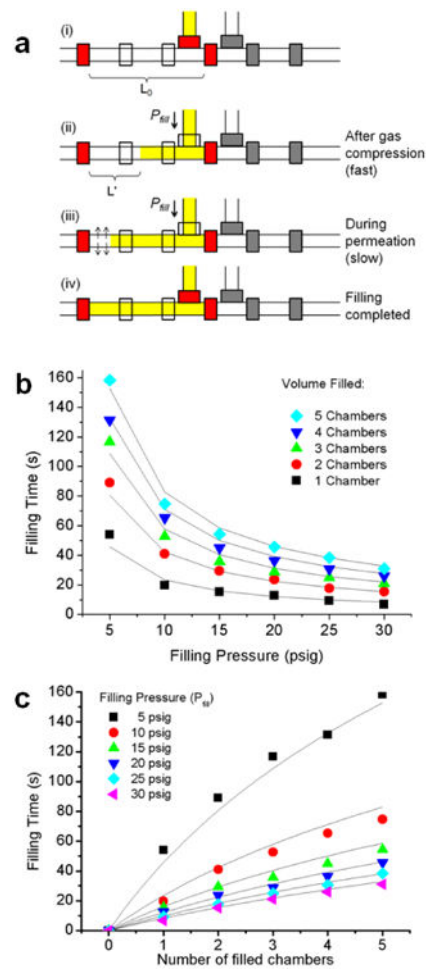


Figure 3. Three methods of programming slug size and composition. *Scheme 1:* Reagents A and B are filled from the center of the slug generator. Reagent A fills 0-5 chamber volumes to the left of V_{iso} and Reagent B fills 0-5 chamber volumes to the right of V_{iso} . The three examples show A:B ratios of 1:1, 3:1, and 1:5. *Scheme 2:* Reagents A and B are filled from the center and buffer solutions fill the remainder of the 5 chambers on each side of V_{iso} to ensure uniform slug size. The composition (ratio of A:B) can be varied over the same range as Scheme 1, but concentrations of A and B relative to original stock solutions are limited to 0, 10, 20, 30, 40, or 50%. *Scheme 3:* Reagents A and B are filled from the ends of the slug generator (i.e. using the buffer inlets) up to an isolation valve (can be any of V_{AX} , V_{BX} , where $X = \{1,2,3,4,5\}$ or V_{iso}). More extreme ratios of reagents are possible than the above cases, but the slug size must always be 10 unit volumes to ensure the reagents can be merged. All of these techniques can be generalized to any number of chambers.

**Figure 4.**

(a) Schematic of the filling process. Gas initially in chamber (i) is rapidly compressed as filling begins (ii) with a timescale on the order of 100 ms. Trapped, compressed gas permeates out through the PDMS (iii) with a timescale on the order of 1 min until the chamber is filled (iv). (b) Dependence of filling time on the filling pressure, P_{fill} , for several different slug sizes (number of unit chambers). (c) The same data as (b) but plotted to illustrate dependence of filling time on number of chambers, for several different filling pressures. Points represent experimental data, lines represent non-linear regression fit to a filling model. (Operating conditions: $P_{eject} = 10$ psig [69 kPag], vent time = 200 ms.)

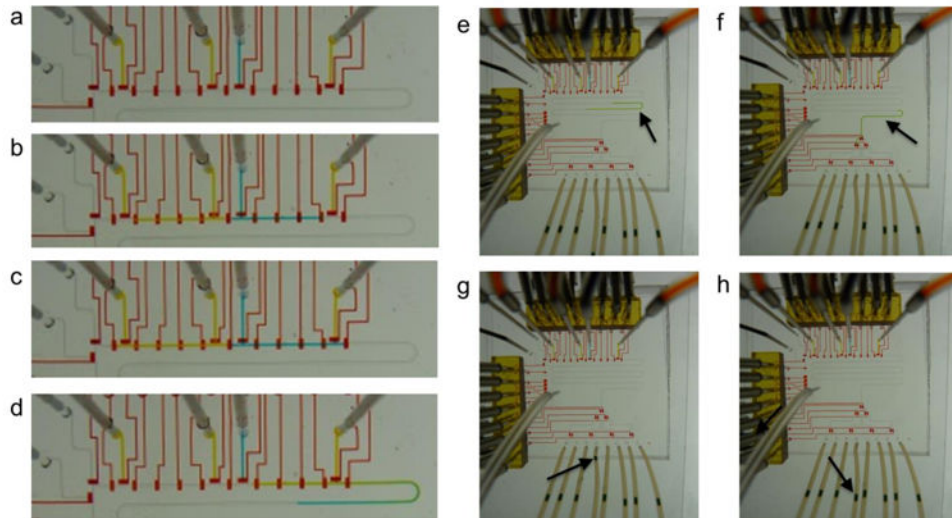


Figure 5. Time sequence of micrographs of a two-component slug being generated, then ejected and pumped through the mixing channel. (a) Chamber volumes are selected by choice of valve states; (b) Chambers are filled; (c) Chambers are merged to form a contiguous slug; (d) Slug is ejected; (e-h) Slug is pumped through mixing channel and then to the pre-selected output port into the output tubing.

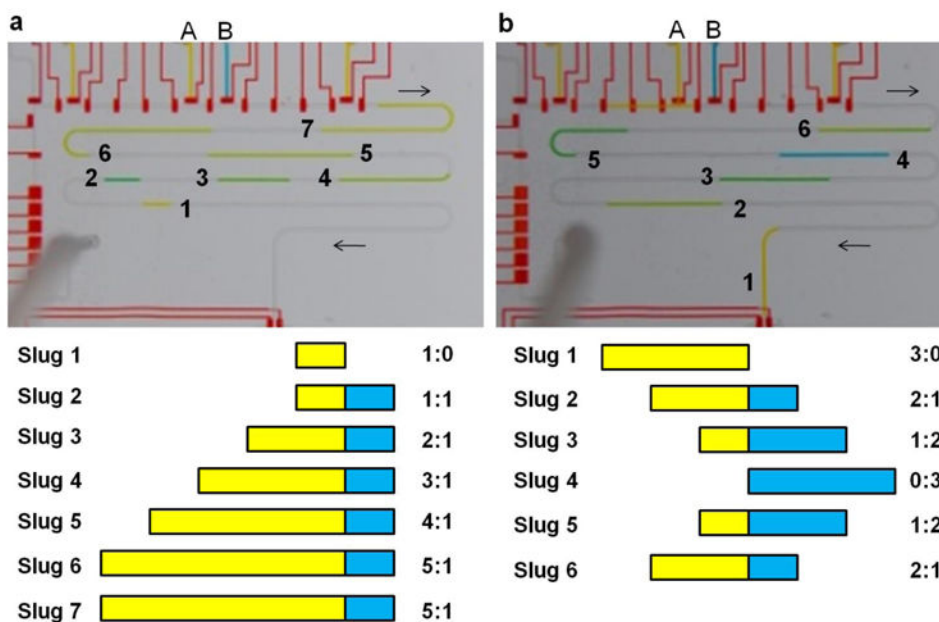


Figure 6. Generation of successive slugs of two reagents (A and B) having different composition selected in real-time. Reagents were loaded from the center and buffer inlets were not used. The slug ejection time was shortened for this image to ensure all slugs fit into the mixing channel. It is evident that the slugs are already well-mixed after traveling a short distance along the channel. (a) Slugs with varying size and composition; (b) Slugs with constant volume (3 unit volumes) but varying composition. Below each image is a schematic representation of the slug composition and numerical ratio of reagent A (yellow) and reagent B (blue).

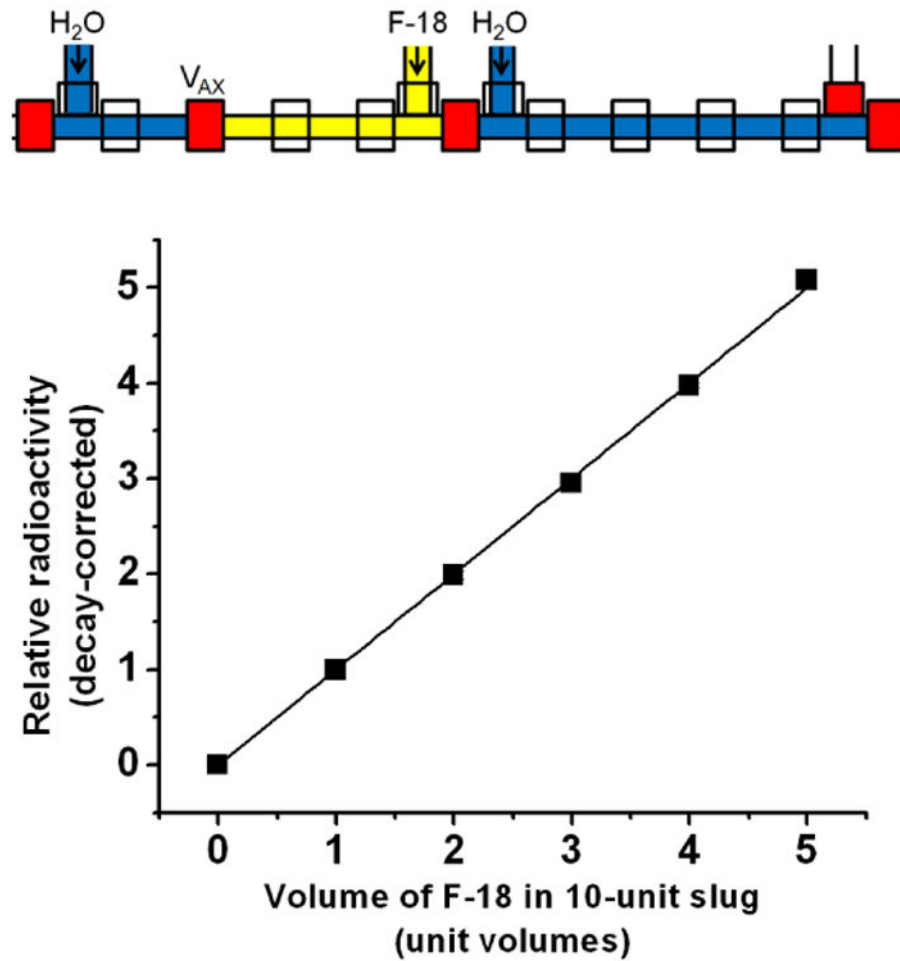


Figure 7. Validation of volume ratio accuracy. (Top) Schematic of generation of slugs containing [F-18]fluoride solution. 10-unit-volume slugs containing $X = 0$ to 5 unit volumes of [F-18]fluoride solution were generated. Each slug was collected and its radioactivity measured and corrected for radioactive decay ($t_{1/2} = 110$ min). Ratio of radioactivities of $X = \{0, 2, 3, 4, 5\}$ slugs to $X = 1$ slugs were computed. The experiment was repeated 3 times and the results averaged. The expected results are shown as a continuous line. Ratio of volumes matches expected values within $<1.6\%$.